RESEARCH PAPER

Influence of pore pressure on plastic deformation and strength of limestone under compressive stress

B. Han[1,2] · W. Q. Shen[2] · S. Y. Xie[2] · J. F. Shao[1,2]

Abstract

This study is devoted to experimental investigation of effects of pore pressure on plastic deformation and failure of a water-saturated limestone. The experimental study is composed of three different groups of laboratory tests. The basic mechanical behavior of the rock is first characterized by drained triaxial compression tests on water-saturated samples without pore pressure. The results are compared with those obtained in a previous study from triaxial compression tests on saturated samples with a constant pore pressure. In the second group, water injection tests under a confining pressure of 20 MPa and different values of deviatoric stress are realized to study the effect of pore pressure increase. Finally, undrained triaxial compression tests are carried out for investigating the coupling effect of plastic deformation and pore pressure variation. Based on experimental data, the validity of effective stress concept for plastic yielding and failure strength is discussed.

Keywords Effective stress · Limestone · Plastic deformation · Poroelasticity · Pore pressure · Porous rocks

1 Introduction

Porous rocks are generally saturated by one or several fluids. Under mechanical loading and temperature change, important variation of pore pressure can be generated. For many engineering applications, it is important to study effects of pore pressure on deformation behavior and mechanical strength of porous rocks. Since the Biot's theory of poroelasticity [2], a great number of studies have been performed on experimental investigation of elastic behavior of saturated porous rocks. The poroelasticity has been extended to nonlinear rheology [3], anisotropic materials [6, 8, 35], to materials with induced damage by microcracks [32, 45, 48]. Different experimental techniques have been proposed for the measurement of poroelastic parameters in saturated porous materials [4, 15, 17, 20, 29]. Poroelastic theory has also been successively applied to the analysis of deformation, instability and failure in various engineering contexts [26]. Some studies have been devoted to undrained poroelastic response to deviatoric stress change and to effect of temperature-induced pore pressure on the strength of porous rocks [21, 22]. Using homogenization techniques, poroelastic coefficients have been determined as responses of microstructure [12, 23].

On the other hand, most porous rocks also exhibit plastic deformation. Extensive experimental studies are available on the characterization of plastic deformation in porous rocks [1, 11, 16, 33, 39, 42]. In general, two plastic deformation processes can be identified, the irreversible collapse of voids and the plastic shearing related to frictional sliding between mineral grains. The plastic behavior of porous rocks is also strongly influenced by confining pressure. There is a clear transition from brittle to ductile behavior when the confining pressure increases [5, 28, 40]. Various constitutive models have also been developed for porous rocks. In general, one can find models either with a single yield surface or with two distinct yield surfaces to describe the two plastic processes. However, the description of plastic deformation and failure strength with pores pressure variation in porous materials is still an open issue.

✉ J. F. Shao
jian-fu.shao@polytech-lille.fr

1 College of Civil Engineering and Architecture, Hubei University of Technology, Wuhan 430068, China

2 CNRS, LaMcube, FRE 2016, University of Lille, 59000 Lille, France

A number of previous studies have been so far performed to investigate effects of pore pressure variation on plastic yielding, earthquake rupture dynamics, nucleation of slip-weakening rupture instability and other features [13, 14, 19, 36, 37, 46, 48]. The concept of effective stress is generally involved for both elastic and plastic fields [7, 34, 43, 47]. However, the existence and validity of effective stress concept for plastic deformation and failure strength in saturated and partially saturated materials are still an open issue [9, 19, 38, 42, 46]. With the help of nonlinear homogenization techniques, some micro-mechanical studies have been reported on the effective stress concept for plastic yield and strength criteria in saturated materials [10, 24]. In addition, one can also find experimental studies on chemical effects of pore fluids on mechanical properties of porous rocks [7, 16, 31, 41, 44]. It is found that the plastic yield and strength criteria are affected by physical and chemical processes in pore fluids such as dissolution, wettability, capillary force and other factors.

In our previous study [14], we have investigated the basic mechanical behavior and the effect of plastic deformation on the permeability evolution of a saturated limestone in drained triaxial compression tests with a constant pore pressure of 5 MPa. As an extension to the previous study, the objective of this paper is to study the effect of constant or varying pore pressure on plastic deformation and failure strength of saturated porous rocks by performing a series of new laboratory tests. For this purpose, the same limestone as that used in Han et al. [14] is selected in the present work. The experimental program is composed of three groups of laboratory tests. A series of drained triaxial compression tests are first performed on water-saturated samples without pore pressure but with different values of confining pressure, which are chosen in a special way so that the values of effective confining pressure (defined as the difference between confining pressure and pore pressure) are the same as those used in the previous study. The effect of a constant pore pressure on plastic deformation and failure strength is therefore discussed. Then, another series of triaxial compression tests are carried out by injecting water into samples at different levels of deviatoric stress. The objective is to investigate the consequence of pore pressure increase on plastic deformation and failure. Finally, undrained triaxial compression tests are realized in order to study the coupling effect between plastic deformation and pore pressure variation.

2 Experimental procedure and results

The present study is performed on Anstrude limestone from Bourgogne in France. This rock has been previously investigated by Lion et al. [20] and Han et al. [14]. The lithology, microstructure and mineralogy of this rock have been characterized in the previous papers. Anstrude limestone is composed of about 98% calcite and 2% quartz, with an average porosity of 20% and an initial permeability of about 6×10^{-16} m^2. The experimental scatter is a common phenomenon in laboratory tests. It is mainly caused by the natural scatter of samples and by the differences of testing procedure. In order to reduce the experimental scatter, the tests presented in this paper are carried out with the same procedures. The hard task is to reduce the natural scatter of samples. For this purpose, the samples used in the previous study of Han et al. [14] and in the present study are all carefully drilled from a homogeneous block without macroscopic cracks. If some abnormal results are obtained from a test, a second test is performed to verify the results.

The following methodology is adopted. The basic mechanical behavior of Anstrude limestone has been studied in Han et al. [14] through a series of drained triaxial compression tests on saturated samples with a constant pore pressure of 5 MPa. In the present work, the emphasis is put on the effect of pore pressure on plastic deformation and failure strength of the limestone. For this purpose, three groups of laboratory tests will be performed. In the first group, drained triaxial compression tests are performed on saturated samples without pore pressure. (Or the pore pressure is equal to zero.) The values of confining pressure are especially selected so that the values of effective confining pressure, which is defined as the difference between nominal confining pressure and pore pressure, are identical for two series of tests, respectively, performed with 0 and 5 MPa pore pressure. In this way, we shall identify the effect of a constant pore pressure on plastic deformation and failure strength of limestone. In the second group of tests, the pore pressure is increased by injecting water into samples at different levels of deviatoric stress until failure at a selected confining pressure. The purpose of these tests is to investigate the mechanical responses of limestone to pore pressure increase. Finally, in the third group, a series of undrained triaxial compression tests are realized with different confining pressures in order to capture the coupling process between the evolution of pore pressure during deviatoric stress loading, plastic deformation and failure behavior.

All the tests are performed using a custom-designed autonomous and auto-compensated triaxial testing device. This is mainly composed of a cylindrical cell and three

pressure generators and a computer monitoring system. It is possible to independently apply and monitor confining pressure, axial stress, inlet and outlet pore pressures. The axial strain is measured by two LVDT transducers, which are placed between the bottom and top platens inside the cell. The radial (or lateral) strain is measured by a custom-designed strain ring placed at the middle height of sample. The detailed presentation of the device and strain measurement techniques was given in Han et al. [14]. All the samples, used in the previous study [14] and in this study, were carefully drilled from a big block without macroscopic cracks and homogeneous at the sample scale. The size of cylindrical samples is 37.5 mm in diameter and 75 mm in length. All tests will be performed in a room with a temperature controlled around 20 ± 2 °C.

2.1 Triaxial compression tests with a constant pore pressure

The drained triaxial tests with a constant pore pressure are performed by three steps. The confining pressure (noted as $P_c = \sigma_3$) is increased to a selected value in the first step. The pore pressure (noted as P_i) is then increased by water injection to a desired value in the second step. At the third step, the axial stress (noted as σ_1) is finally applied with a given axial strain rate (noted as $d\varepsilon_1/dt$) in order to capture post-peak response of sample. The axial strain rate is chosen as slow as possible so that the over-pore pressure does not create a significant disturbance of the prescribed uniform pore pressure inside the sample. In the present study, the axial strain rate was selected as 5×10^{-6}/s. Note that in the previous study [14], a series of drained triaxial compression tests with a constant pore pressure of $P_i = 5$ MPa have been performed with seven different confining pressures such as 8, 11, 15, 20, 30, 40 and 55 MPa. In order to capture the effect of a constant pore pressure, in the present study, drained triaxial compression tests are performed on saturated samples but without pore pressure ($P_i = 0$ MPa). Seven specific values of confining pressure are selected: 3, 6, 10, 15, 25, 35 and 50 MPa. These values are selected in a way that the effective confining pressures defined as the difference between confining pressure and pore pressure ($P_c - P_i$) are identical for the two series of tests, respectively, performed in the previous and present studies. Therefore, the results obtained from the two series of tests can be compared and their differences can be used to interpret the effect of pore pressure. In Fig. 1, we present the deviatoric stress defined as ($\sigma_1 - \sigma_3$) versus the axial strain and lateral strain (noted as ε_3). In this figure, the stress–strain curves are presented in two separate groups, respectively, for "low" and "high" confining pressures. The definition of low and high confining pressures is relatively subjective and mainly based on the general trend of
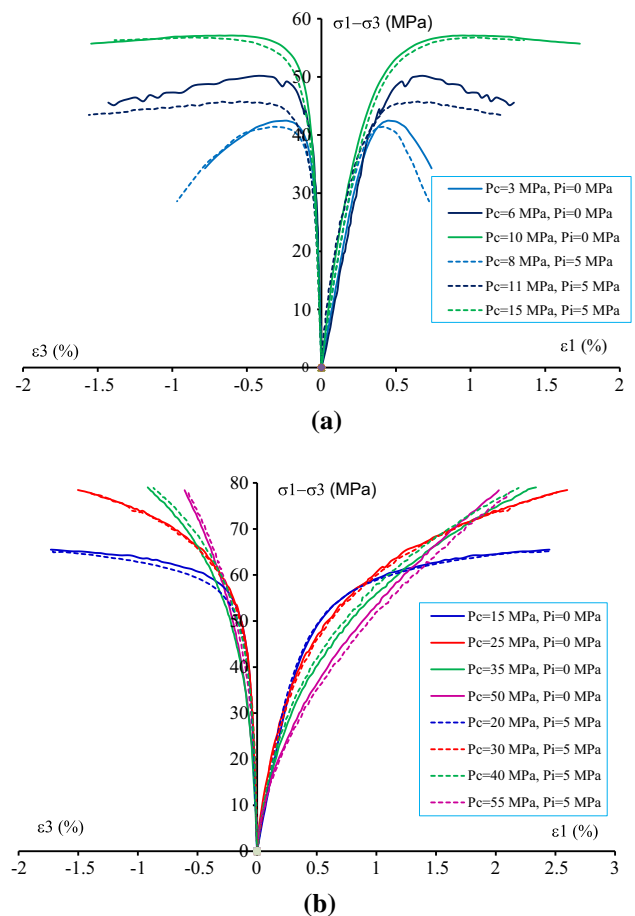

Fig. 1 Comparisons of stress–strain curves between drained triaxial compression tests with a constant pore pressure ($P_i = 5$ MPa) [14] and without pore pressure ($P_i = 0$). **a** 'Low' confining pressures, **b** 'high' confining pressures

mechanical behavior. For the tests under "low" confining pressures, the basic behavior of limestone is typically elastic brittle or elastoplastic brittle, and the failure state of sample can be clearly identified by a peak stress. In contrast, for the tests under "high" confining pressures, the basic behavior of limestone is elastoplastic ductile, and no peak stress can be defined until a relatively large axial strain. Detailed discussions on the effect of constant pore pressure will be given in the next section.

2.2 Water injection tests

In these tests, the sample is first subjected to a classical drained triaxial compression loading without initial pore pressure. When the deviatoric stress reaches a selected value and the strains become stable (green points in Fig. 2), an increase in pore pressure is generated by injecting water into the sample until the peak deviatoric stress is obtained (blue points in Fig. 2). After the peak stress, the water injection is continued with the same flow rate and the axial
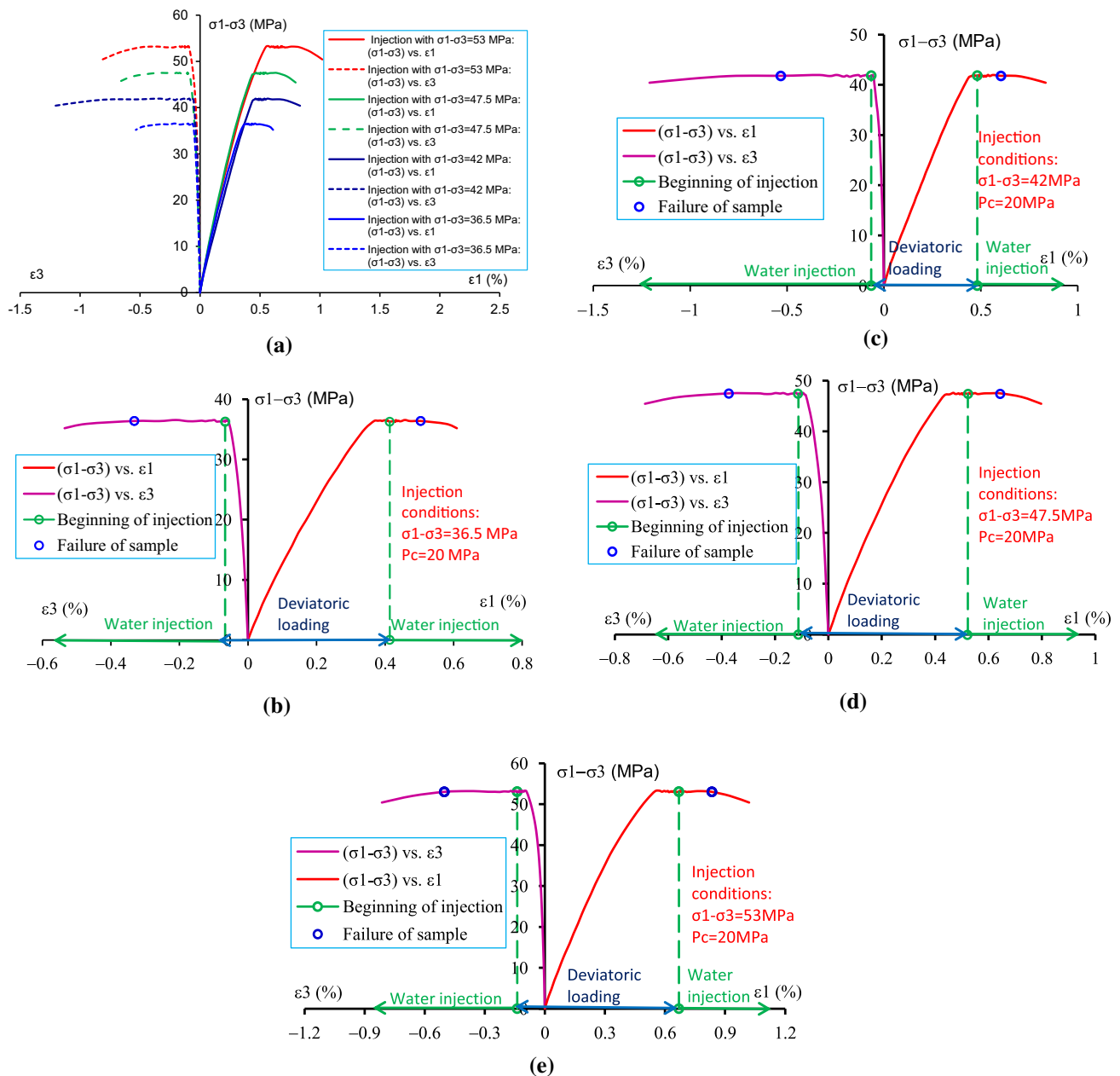
Fig. 2 Overall curves (**a**) and individual curves (**b**–**e**) of deviatoric stress versus axial and lateral strains during triaxial compression tests with water injection at different values of deviatoric stress and under a confining pressure of 20 MPa

strain is controlled by the corresponding pressure generator. It is thus possible to capture the post-peak behavior of sample during the water injection test (after the blue points in Fig. 2). Four tests are performed under a confining pressure of 20 MPa and with the deviatoric stresses of 36.5, 42.0, 47.5 and 53 MPa, respectively. The water is injected from the inlet point, while the outlet point is closed. The water injection flow rate is 0.003 ml/s. Both the inlet and outlet pressures are measured during the injection. The inlet pore pressure is slightly higher than the outlet one, but the difference is less than 0.1 MPa due to the relatively

high permeability of limestone and the small injection rate. The overall and individual curves of deviatoric stress versus axial and lateral strains are presented in Fig. 2. The variations of pore pressure are shown as functions of the axial and lateral strains in Fig. 3.

2.3 Undrained triaxial compression tests

The undrained triaxial compression test is performed in three steps. The selected confining pressure is first applied. An initial pore pressure is then set up in order to insure a
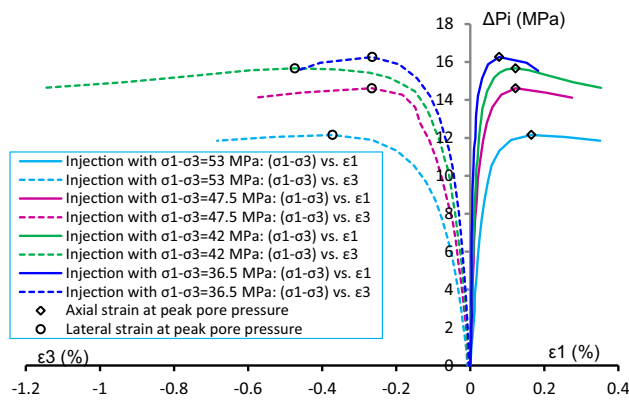
Fig. 3 Variations of axial and lateral strains with pore pressure increase during triaxial compression tests with water injection phase at different values of deviatoric stress and under a confining pressure of 20 MPa

good saturation state and to better measure variation of pore pressure during test. Finally, the axial stress is applied while the pore fluid circuit is closed from the exterior of sample. Fours tests are performed with four different confining pressures (6, 10, 23 and 38 MPa) and an initial pore pressure of 3 MPa. The axial strain rate is the same as that used in drained tests. In Fig. 4, we present the deviatoric stress versus the axial and lateral strains as well as the pore pressure, respectively.

3 Effects of pore pressure

As discussed in the previous study [14], the basic mechanical behavior of Anstrude limestone is characterized by two plastic deformation processes: pore collapse and plastic shearing. The effective mean stress threshold for pore collapse is about 44 MPa. Under low effective confining pressures (3, 6 and 10 MPa), the plastic shearing is the dominant process producing the strain softening in the post-peak regime and volumetric dilatancy. On the other hand, under high effective confining pressures (25, 35 and 50 MPa), the pore collapse plays an essential role and is responsible for volumetric compaction and ductile failure process. For an intermediate effective confining pressure such 15 MPa, there is a competition between the two plastic processes and it represents the transition point from brittle to ductile behavior of material. In this section, we shall discuss the effect of a constant pressure on two plastic deformation processes and failure strength of limestone.

3.1 Influence of a constant pore pressure

According to Fig. 1, for the effective confining pressures higher than 10 MPa, the stress–strain curves obtained, respectively, from tests without pore pressure and those
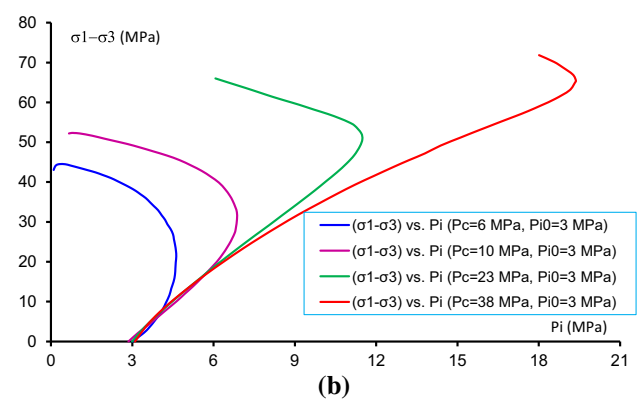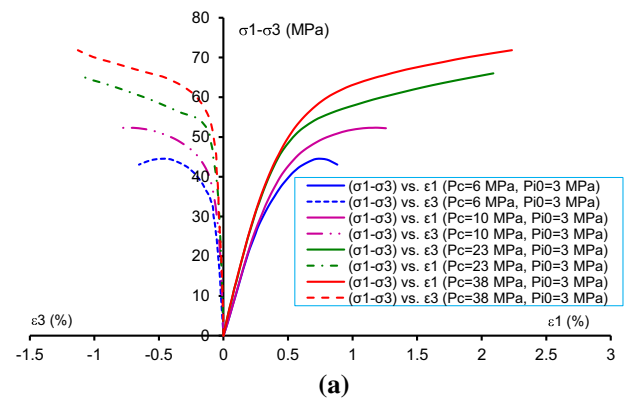

Fig. 4 Deviatoric stress versus axial and lateral strains as well as pore pressure in undrained triaxial compression tests with different confining pressures and an initial pore pressure of 3 MPa. **a** Deviatoric stress versus axial and lateral strains, **b** deviatoric stress versus pore pressure

with a constant pore pressure of 5 MPa [14] are nearly identical. However, for two low effective confining pressures (3 and 6 MPa), it seems that the peak deviatoric stress of samples with pore pressure is slightly lower than that of samples without pore pressure for a same value of effective confining pressure. In order to quantity the effect of pore pressure, we have determined the stress threshold, respectively, for the initial plastic shearing in the tests with low confining pressures, the pore collapse and onset of plastic shearing in the tests under high confining pressures. Under a low confining pressure, after the elastic limit, there is a clear transition from volumetric compressibility to dilatancy during the deviatoric loading. In order to better investigate the plastic volumetric strain transition, an elastic reference line is added on the basis of the extrapolation of the approximately linear part of the deviatoric stress versus volumetric strain curve. It is found that the plastic volumetric dilatancy threshold nearly coincides with the plastic shearing threshold. Under a high confining pressure, after the elastic limit stress, there is an important volumetric compaction due to the plastic pore collapse, followed by a clear transition from compaction to
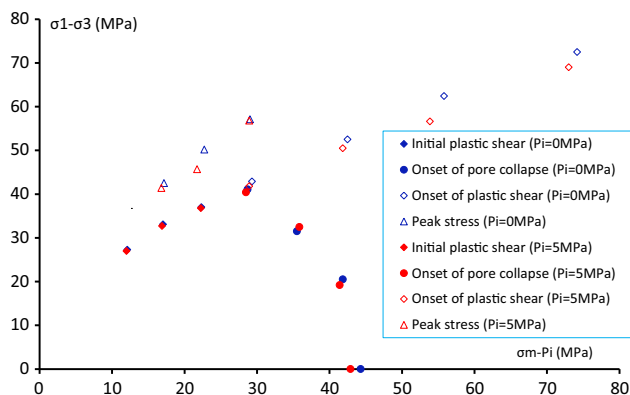
Fig. 5 Comparisons of stress threshold for plastic shearing, pore collapse and peak deviatoric stress obtained in triaxial compression tests without and with pore pressure in the diagram of deviatoric stress versus mean stress ($\sigma_m - p_i$)

dilatancy. Therefore, two reference lines can be added on the deviatoric stress versus volumetric strain curve. The first one defines the elastic strain slope, and the second line defines the average slope of the quasi-linear part of the curve during the pore collapse process. With the help of these two lines, it is easy to identify the pore collapse threshold and the plastic shearing threshold. The more detailed description for the determination of the onset points was presented in Han et al. [14]. The obtained results are presented in the diagram of deviatoric stress versus effective mean stress ($\sigma_m - P_i$, $\sigma_m = (\sigma_1 + 2\sigma_3)/3$), as shown in Fig. 5. Except the small difference of peak strength mentioned before, the onset of pore collapse and plastic shearing are almost not affected by the pore pressure. These results indicate that the mechanical behavior of limestone in triaxial compression tests is approximately controlled by the effective confining pressure defined according to the effective stress of Terzaghi. More detailed discussions about the effective stress concept will be given in the next section.

3.2 Analysis of water injection tests

In Fig. 6, the loading paths during the water injection tests are indicated by the horizontal lines in the diagram of deviatoric stress ($\sigma_1 - \sigma_3$) versus effective mean stress ($\sigma_m - P_i$). In this figure, the initial shearing threshold surface, the pore collapse surface and the peak strength surface are also illustrated. The corresponding variations of axial and lateral strains are presented in Fig. 3. It is seen that the mechanical responses of limestone during the water injection phase are dependent on the values of deviatoric stress of injection point, respectively, equal to 36.5, 42, 47.5 and 53 MPa. When the deviatoric stress is low, e.g., 36.5 MPa, the water injection point is in the elastic domain. The water injection process should generate

elastic tensile strains at both the axial and lateral directions. This is the case for the lateral strain as shown in Fig. 3. However, one gets a compressive axial strain. This is not verified by the isotropic poroelastic theory. There are several possible reasons to explain such a compressive strain induced by the water injection. Based on some previous studies [27], the water injection can enhance the pressure solution process in limestone and induce a weakening of both elastic modulus and mechanical strength of material. Therefore, if such a weakening effect exists, the water injection can induce a decrease in plastic yield stress of limestone and then generate additional plastic strains. Due to the applied deviatoric stress, the additional axial plastic strain should be compressive. However, additional investigations are needed to confirm the weakening effect of water injection in limestone. With the increase in pore pressure due to water injection (moving to the left on the diagram), the plastic shearing surface is reached as shown in Fig. 3. When the peak strength surface is finally reached, there is a material softening and a diminution of pore pressure. Moreover, the diminution of pores pressure is directly related to an important volumetric dilatancy. For higher levels of deviatoric stress (42, 47.5 and 53 MPa), the injection point is behind the initial pore collapse surface. This means that the material is in the plastic domain when the water injection is started. However, during the water injection phase, due to the increase in pore pressure before peak strength, there is an elastic unloading with respect to the pore collapse surface. However, when the plastic shearing surface is reached, the plastic deformation occurs but only due to the shearing process. Therefore, the plastic deformation during the water injection phase is dominated by the plastic shearing process.

3.3 Analysis of undrained tests

In Fig. 7, we present the curves of deviatoric stress versus axial and lateral strains as well as pore pressure versus axial strain separately for each value of confining pressure. In Fig. 8, the stress paths during the undrained tests are illustrated with respect to the initial plastic shearing surface, pore collapse surface and peak strength surface. It can be seen that the mechanical response of limestone during undrained triaxial compression tests is also influenced by confining pressure, in particular in terms of pore pressure, volumetric dilatancy and peak strength.

Let us first consider two tests under a low confining pressure (6 and 10 MPa). In the initial elastic zone, there are quasi-linear relations between strains, pore pressure increase and deviatoric stress. When the plastic shearing surface is reached, plastic deformation occurs with the shearing process. The plastic deformation produces a slight
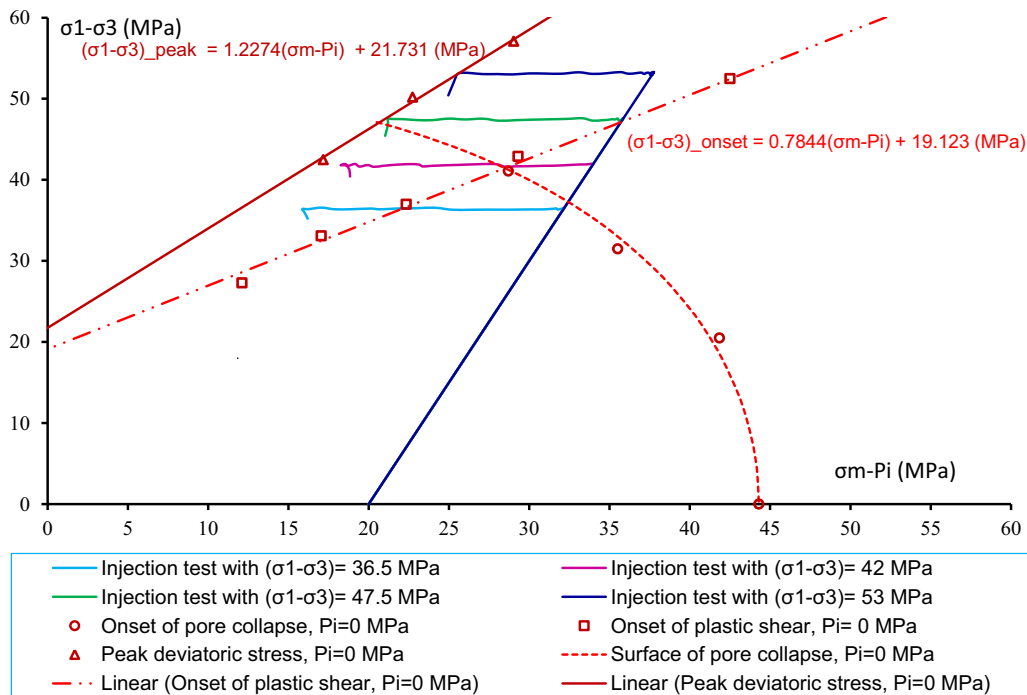
Fig. 6 Stress paths in water injection tests with respect to initial plastic shearing surface, pore collapse surface and peak deviatoric stress surface determined from triaxial compression tests without pore pressure

volumetric dilatancy but the total volumetric strain remains compressive. The pore pressure should continue to increase but with a reduced rate. Some scatters from this theoretical prediction are found on the experimental data obtained. It seems that the pore pressure drop starts before the volumetric compressibility–dilatancy transition point is reached. This may be attributed to possible heterogeneous distribution of pore pressure inside the sample. After the onset of volumetric dilatancy, the plastic strains become more significant and the pore pressure decreases quickly. The peak strength surface is then reached, and the peak deviatoric stress is obtained. The peak strength is more pronounced when the confining pressure is lower, and this indicates the transition from brittle to ductile behavior. The pore pressure continues to decrease during the post-peak regime and finally approaches zero. One obtains some residual stress–strain regime. Note that in these two tests, the pore collapse surface is never reached. Therefore, the plastic deformation is entirely controlled by the shearing process.

For the test under a high confining pressure (38 MPa), after an initial elastic phase, the plastic pore collapse surface is reached before reaching the shearing surface. The two plastic processes have a competitive influence on pore pressure evolution. The pore collapse process produces a volumetric compaction. As a consequence, one gets a significant increase in pore pressure. When the plastic shearing is reached, a volumetric dilatancy is produced and

the rate of pore pressure increase is reduced. The volumetric compressibility–dilatancy transition is then observed, and one observes a quasi-constant phase of pore pressure. Finally, the pore pressure decreases with the increase in volumetric dilatancy. In this case, the plastic pore collapse process plays an essential role in the pore pressure evolution while the material failure is controlled by the plastic shearing.

For the test with an intermediate confining pressure (20 MPa), both two plastic processes are also activated. However, the plastic shearing is reached before the plastic pore collapse. Even if the plastic shearing process produces a volumetric dilatancy, the overall volumetric strain remains compacting and the pore pressure continues to increase. Progressively, the plastic shearing process becomes dominant with respect to pore collapse. One obtains the transition from compressibility to dilatancy and the decrease in pore pressure.

4 Discussions

The presence of fluid can affect the mechanical behavior of rock through both chemical and mechanical interactions [28]. As mentioned above, there are some differences of plastic yield and failure surfaces between tests without and with pore pressure. For a better understanding of such differences, the experimental results obtained are now
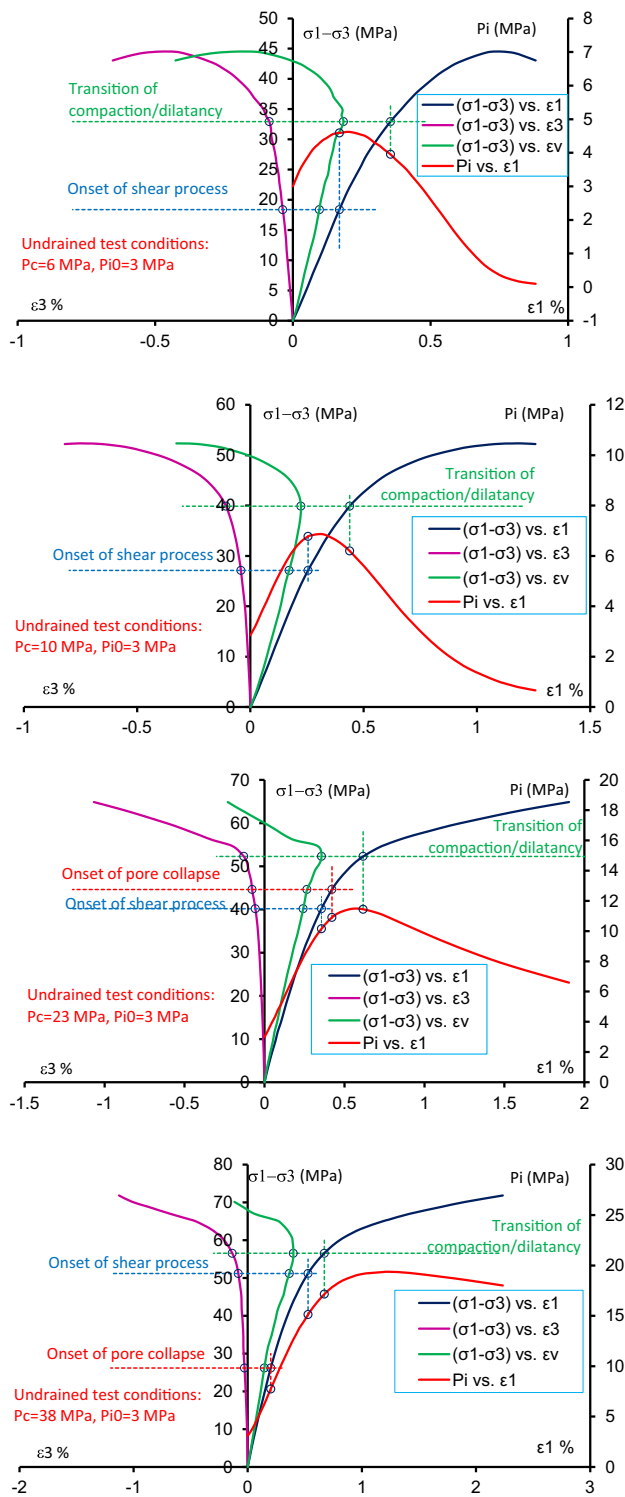
Fig. 7 Variations of strains and pore pressure in undrained triaxial compression tests under different confining pressures and an initial pore pressure of 3 MPa

analyzed in terms of effective stress concept and chemical effect of pore fluid.

4.1 Discussion on effective stress concept for plasticity

Based on a macroscopic kinematic assumption, Coussy [8] has introduced the concept of effective stress for poroelasticity theory by the relation $\sigma_{ij}^p = \sigma_{ij} - \beta p \delta_{ij}$, with $\beta \leq 1$ being the plastic effective stress coefficient, which is physically different with the Biot's coefficient for poroelasticity theory.

In Fig. 5, the threshold stresses for plastic shearing, pore collapse and peak strength are presented, respectively, from the tests without pore pressure ($p_i = 0$) and with a constant pore pressure ($p_i = 5$ MPa). One can see that the pore collapse threshold obtained from the test with $p_i = 5$ MPa is slightly lower than that from the test with $p_i = 0$. By assuming the validity of plastic effective stress concept and by neglecting for the moment any chemical effect of water on limestone, one can easily deduce $\beta < 1$ for the studied limestone. Following this concept, the effective confining pressure ($P_c - \beta p_i$) in a test with $P_{c1}, p_i > 0$ should be higher than that in a test with $P_{c2}, p_i = 0$ if $P_{c1} - p_i = P_{c2}$. As a consequence, the plastic shearing threshold for the test with $p_i > 0$ should be higher than that of the test with $p_i = 0$. This theoretical prediction is not verified by the experimental data in Fig. 5. Indeed, the initial plastic shearing surface issued from tests with $p_i = 5$ MPa is slightly lower than that issued from those with $p_i = 0$. A similar result can be obtained about the peak strength surface. The peak strength of samples with pore pressure is generally lower than that in samples without pore pressure. The stress paths followed in the water injection tests are shown in Fig. 6. One can make the same remark as the tests with a constant pressure. For instance, for the tests performed with low deviatoric stress levels (36.5 and 42 MPa), it is clear that the peak deviatoric stresses obtained in the water injection tests are lower than that obtained the triaxial compression tests without pore pressure. As a conclusion, it seems that the effect of pore pressure on plastic deformation and strength cannot be explained by the mechanical effect only. It seems that the presence of pore fluid induces a chemical degradation which affects both plastic yield stress and peak strength.

4.2 Discussion on degradation effect of pore pressure

The objective here is not to present a detailed study on physical and chemical reactions between water and limestone. We just want to discuss the effects of pore pressure increase on plastic deformation and strength of limestone. However, it is useful to mention some possible physical and chemical processes between water and limestone
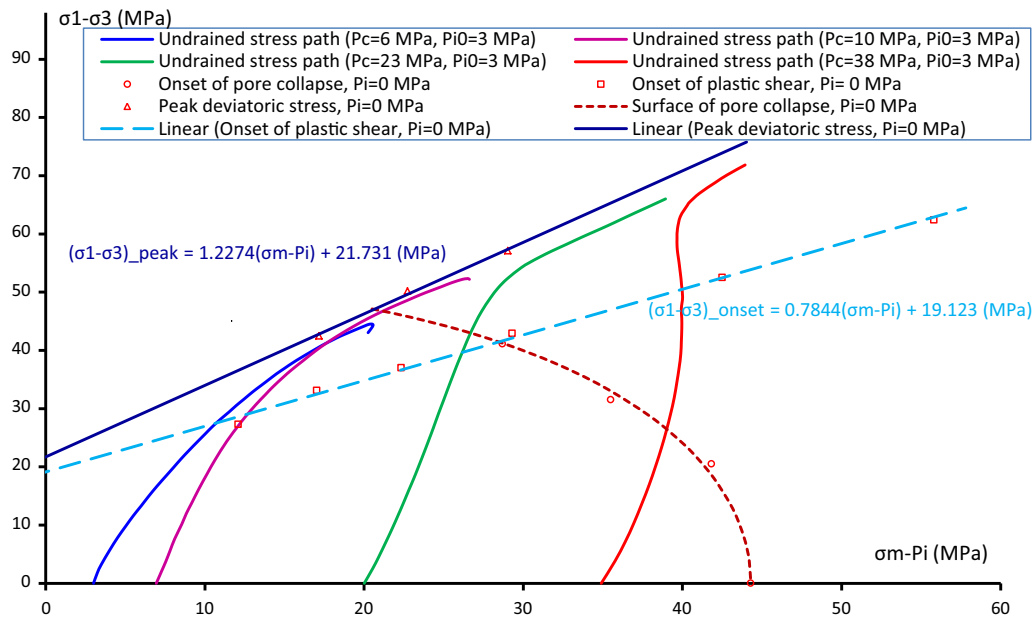
Fig. 8 Stress paths in undrained triaxial compression tests with respect to initial plastic shearing surface, pore collapse surface and peak deviatoric stress surface determined from triaxial compression tests without pore pressure

observed in some previous studies. One can invoke the dissolution of contact surfaces by the inter-granular pressure solution [18, 25, 30, 31, 44]. It was found that the effect of chemical dissolution is generally amplified by the increase in pore pressure [27]. For the limestone studied here, as presented above, under a low effective confining pressure, the mechanical behavior of limestone is clearly affected by the increase in pore pressure. In contrast, the mechanical behavior under a high effective confining pressure seems not affected by the increase in pore pressure. In order to confirm this result with a higher pore pressure, we have performed two additional triaxial compression tests with a constant pore pressure of 18 MPa and two confining pressures of 33 and 53 MPa, respectively. In Fig. 9, the obtained results are compared with those obtained from the tests with P_c = 15 MPa, p_i = 0 and P_c = 20 MPa, p_i = 5 MPa, and with P_c = 35 MPa, p_i = 0 and P_c = 40 MPa, p_i = 5 MPa, respectively. It is clear that the peak strength for the test with P_c = 33 MPa, p_i = 18 MPa is lower than that with P_c = 20 MPa, p_i = 5 MPa, which is again lower than that with P_c = 15 MPa, p_i = 0, as shown in the deviatoric stress–volumetric strain curves. For the three tests with an effective confining pressure of 35 MPa, the deviatoric stress versus axial strain curves are almost identical. However, the deviatoric stress versus volumetric strain curves show a clear difference. It is clear that the compaction–dilatation transition for the test with P_c = 53 MPa, p_i = 18 MPa is lower than that with P_c = 40 MPa, p_i = 5 MPa, which is again lower than that with P_c = 35 MPa, p_i = 0. At the same time, the plastic

volumetric strain due to pore collapse is amplified by the increase in pore pressure. Therefore, the presence of pore fluid could induce a degradation effect on the plastic yielding and failure strength of limestone and this degradation effect is amplified when the pore pressure is higher.

5 Conclusions

Effects of pore pressure on both plastic deformation and strength of saturated limestone have been investigated in this work. The experimental results have confirmed that the plastic deformation is characterized by pore collapse and shearing. The pore collapse is responsible for volumetric compaction, while the shearing induces a volumetric dilatancy. The plastic deformation is dominated by the pore collapse process under high confining pressures but by the shearing process under low ones. There is a transition from brittle to ductile behavior with the increase in confining pressure.

The water injection induces an increase in pore pressure and then a decrease in effective confining pressure. This enhances the plastic shearing process, volumetric dilatancy and shearing failure. Further only the plastic shearing is activated in such a loading path.

The pore pressure evolution in undrained triaxial tests is also influenced by two plastic processes. At a low confining pressure, the deviatoric stress induces plastic dilatancy due to shearing process and then a decrease in pore pressure. But at a high confining pressure, the deviatoric stress
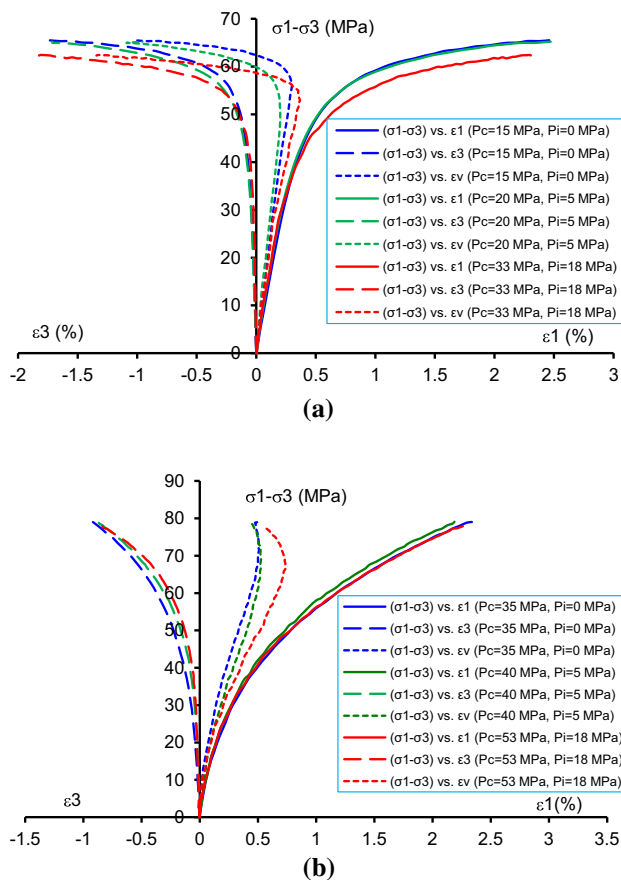
Fig. 9 Stress–strain curves in triaxial compression tests with and without pore pressure but under two same values of $(P_c - P_i)$ for different values of pore pressure (0, 5 and 18 MPa). **a** 'Effective' confining pressure $(P_c - P_i) = 15$ MPa, **b** 'effective' confining pressure $(P_c - P_i) = 35$ MPa

induces a plastic compaction due to pore collapse and enhances the increase in pore pressure. The pore collapse dominates the pore pressure evolution during the first stage of loading, while the plastic shearing dominates the peak strength and pore pressure evolution during the second stage.

The concept of effective stress for plastic deformation and peak strength has been revisited. It is found that the validity of the classical Terzaghi's effective stress concept was not fully verified. The plastic yield stress and peak strength in the samples with pore pressure are generally lower than those in the samples without pore pressure for a same effective confining pressure. It seems that the scatter with the effective stress concept can be attributed to a degradation effect of pore fluid pressure. The presence of pore fluid can induce a decrease in plastic yield stress and peak strength, and the degradation effect is amplified by the increase in pore pressure. However, further investigations are still needed to identify and quantify the origins of degradation effect by pore fluid pressure in limestone.

References

1. Baud P, Schubnel A, Wong TF (1999) Dilatancy, compaction, and failure mode in Solnhofen limestone. J Geophys Res 105(B8):19289–19303
2. Biot MA (1941) General theory of three dimensional consolidation. J Appl Phys 12:155–164
3. Biot MA (1973) Non-linear and semi-linear rheology of porous solids. J Geophys Res 78:4924–4937
4. Boutéca M, Guéguen Y (1999) Mechanical properties of rocks: pore pressure and scale effects. Rev IFP 54(6):703–714
5. Byerlee JD (1968) Brittle–Ductile transition in rocks. J Geophys Res 73(14):4741–4750
6. Cheng AHD (1997) Material coefficients of anisotropic poroelasticity. Int J Rock Mech Min Sci 34(2):199–205
7. Collin F, Cui YJ, Schroeder C, Charlier R (2002) Mechanical behaviour of Lixhe chalk partly saturated by oil and water: experimental and modeling. Int J Numer Anal Methods Geomech 26:897–924
8. Coussy O (1995) Mechanics of porous continua. Wiley, Chichester
9. Coussy O (2004) Poromechanics. Wiley, Hoboken
10. De Buhan P, Dormieux L (1996) On the validity of the effective stress concept for assessing the strength of saturated porous materials: a homogenization approach. J Mech Phys Solids 44:1649–1667
11. De Gennaro V, Delage P, Priol G, Collin F, Cui YJ (2004) On the collapse behaviour of oil reservoir chalk. Géotechnique 54:415–420
12. Dormieux L, Kondo D, Ulm F-J (2006) Microporomechanics. Wiley, Hoboken
13. French ME, Boutt DF, Goodwin LB (2012) Sample dilation and fracture in response to high pore fluid pressure and strain rate in quartz-rich sandstone and siltstone. J Geophys Res 117:B03215. https://doi.org/10.1029/2011JB008707
14. Han B, Xie SY, Shao JF (2016) Experimental investigation on mechanical behavior and permeability evolution of a porous limestone under compression. Rock Mech Rock Eng 49:3425–3435
15. Hart DJ, Wang HF (2001) A single test method for determination of poroelastic constants and flow parameters in rocks with low hydraulic conductivities. Int J Rock Mech Min Sci 38(4):577–583
16. Homand S, Shao JF (2000) Mechanical behaviour of a porous chalk and water/chalk interaction, part I. Experimental study. Oil Gas Sci Technol 55(6):591–598
17. Hu DW, Zhou H, Zhang F, Shao JF (2010) Evolution of poroelastic properties and permeability in damaged sandstone. Int J Rock Mech Min Sci 47(6):962–973
18. Jeschke AA, Dreybrodt W (2002) Dissolution rates of minerals and their relation to surface morphology. Geochim Cosmochim Acta 66(17):3055–3062
19. Kerbouche R, Shao JF, Skoczylas F (1995) On the poroplastic behaviour of porous rock. Eur J Mech A Solids 14:577–587
20. Lion M, Skoczylas F, Ledésert B (2004) Determination of the main hydraulic and poro-elastic properties of a limestone from Bourgogne, France. Int J Rock Mech Min Sci 41:915–925
21. Lisabeth HP, Zhu W (2015) Effect of temperature and pore fluid on the strength of porous limestone. J Geophys Res Solid Earth 120:6191–6208. https://doi.org/10.1002/2015JB012152
22. Lockner DA, Stanchits SA (2002) Undrained poroelastic response of sandstones to deviatoric stress change. J Geophys Res 107(B12):2353. https://doi.org/10.1029/2001JB001460
23. Lydzba D, Shao JF (2000) Study of poroelasticity material coefficients as response of microstructure. Mech Cohesive Frict Mater 5:149–171

24. Lydzba D, Shao JF (2002) Stress equivalence principle for saturated porous media. C R Mécanique 330:297–303

25. Lydzba D, Pietruszczak S, Shao JF (2007) Intergranular pressure solution in chalk; a multiscale approach. Comput Geotech 34:291–305

26. Ma X, Zoback MD (2017) Laboratory experiments simulating poroelastic stress changes associated with depletion and injection in low-porosity sedimentary rocks. J Geophys Res Solid Earth 122:2478–2503. https://doi.org/10.1002/2016JB013668

27. Macdonald RW, North NA (1974) The effect of pressure on the solubility of $CaCO_3$, CaF_2, and $SrSO_4$ in water. Can J Chem 52(18):3181–3186

28. Paterson MS, Wong TF (2005) Experimental rock deformation-the brittle field, 2nd edn. Springer, Berlin

29. Pimienta L, Fortin J, Yves Gueguen Y (2017) New method for measuring compressibility and poroelasticity coefficients in porous and permeable rocks. J Geophys Res Solid Earth 122:2670–2689. https://doi.org/10.1002/2016JB013791

30. Raj R (1982) Creep in polycrystalline aggregates by matter transport through a liquid phase. J Geophys Res 87:4731–4739

31. Risnes R, Madland MV, Hole M, Kwabiah NK (2005) Water weakening of chalk-mechanical effects of water–glycol mixtures. J Petrol Sci Eng 48:21–36

32. Shao JF (1997) Poroelastic behaviour of brittle rock materials with anisotropic damage. Mech Mater 30:41–53

33. Shao JF, Henry JP (1991) Development of an elastoplastic model for porous rock. Int J Plast 7:1–13

34. Stover SC (2003) A one-dimensional analytically based approach for studying poroplastic and viscous consolidation: application to Woodlark Basin, Papua New Guinea. J Geophys Res 108(B9):2448. https://doi.org/10.1029/2001JB000466

35. Thompson M, Willis JR (1991) A reformulation of the equations of anisotropic poroelasticity. J Appl Mech ASME 58:612–616

36. Viesca RC, Rice JR (2012) Nucleation of slip-weakening rupture instability in landslides by localized increase of pore pressure. J Geophys Res 117:B03104. https://doi.org/10.1029/2011JB008866

37. Viesca RC, Templeton EL, Rice JR (2008) Off-fault plasticity and earthquake rupture dynamics: 2. Effects of fluid saturation. J Geophys Res 113:B09307. https://doi.org/10.1029/2007JB005530

38. Warpinski NR, Teufell LW (1993) Laboratory measurements of the effective-stress law for carbonate rocks under deformation. Int J Rock Mech Min Sci Geomech Abstr 30(7):1169–1172

39. Wong TF, Szeto H, Zhang J (1992) Effect of loading path and porosity on the failure mode of porous rocks. Appl Mech Rev 45(8):281–293

40. Wong TF, David C, Zhu W (1997) The transition from brittle faulting to cataclastic flow in porous sandstone: mechanical deformation. J Geophys Res 102:3009–3025

41. Xie SY, Shao JF (2006) Elastoplastic deformation of a porous rock and water interaction. Int J Plast 22:2195–2225

42. Xie SY, Shao JF (2012) Experimental investigation and poroplastic modelling of saturated porous geomaterials. Int J Plast 39:27–45

43. Xie SY, Shao JF (2015) An experimental study and constitutive modeling of saturated porous rocks. Rock Mech Rock Eng 48:223–234

44. Xie SY, Shao JF, Xu WY (2011) Influences of chemical degradation on mechanical behaviour of a limestone. Int J Rock Mech Min Sci 48:741–747

45. Xie N, Zhu QZ, Shao JF, Xu LH (2012) Micromechanical analysis of damage in saturated quasi brittle materials. Int J Solids Struct 49:919–928

46. Yamada SE, Schatz JF, Abou Sayed A, Jones AH (1981) Elastoplastic behavior of porous rock under undrained condition. Int J Rock Mech Min Sci Geomech Abstr 18:177–179

47. Yarushina VM, Podladchikov YY (2015) (De)compaction of porous viscoelastoplastic media: model formulation. J Geophys Res Solid Earth 120:4146–4170. https://doi.org/10.1002/2014JB011258

48. Zhang J, Wong T-F, Davis DM (1990) Micromechanics of pressure-induced grain crushing in porous rocks. J Geophys Res 95:341–352

Publisher's Note